From partons to new physics

Connections between the Standard Model and LHC discoveries

Pavel Nadolsky

Michigan State University

February 13, 2008

Perturbative QCD computations

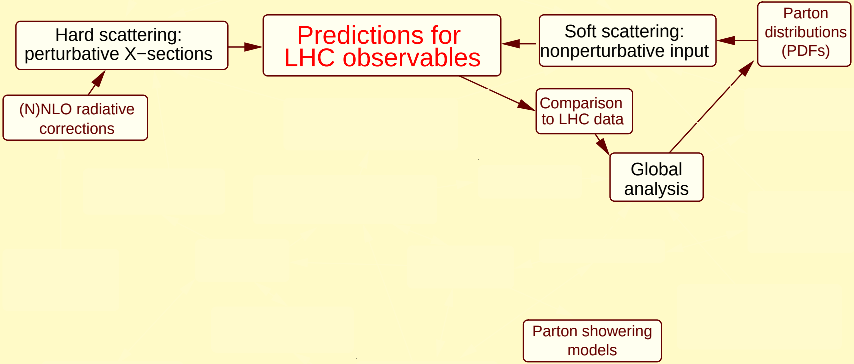

A partial picture

Perturbative QCD computations

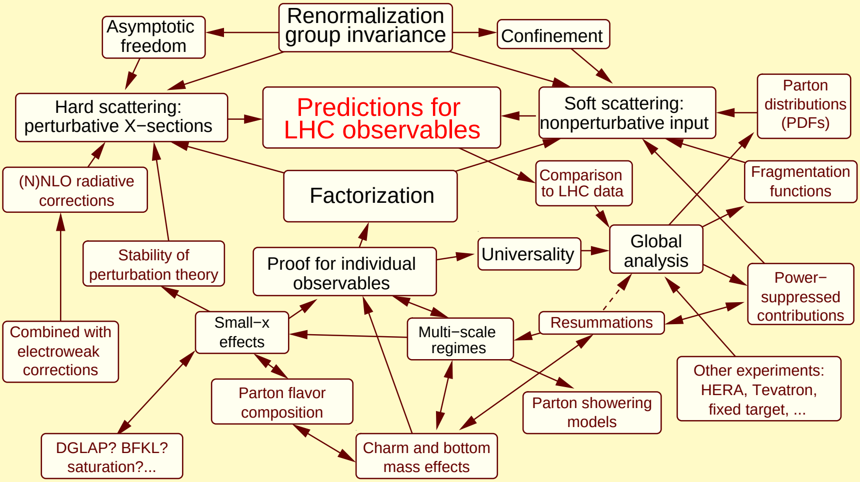

Global interconnections can be as important as (N)NLO perturbative contributions; are different at the Tevatron and LHC

Perturbative QCD computations

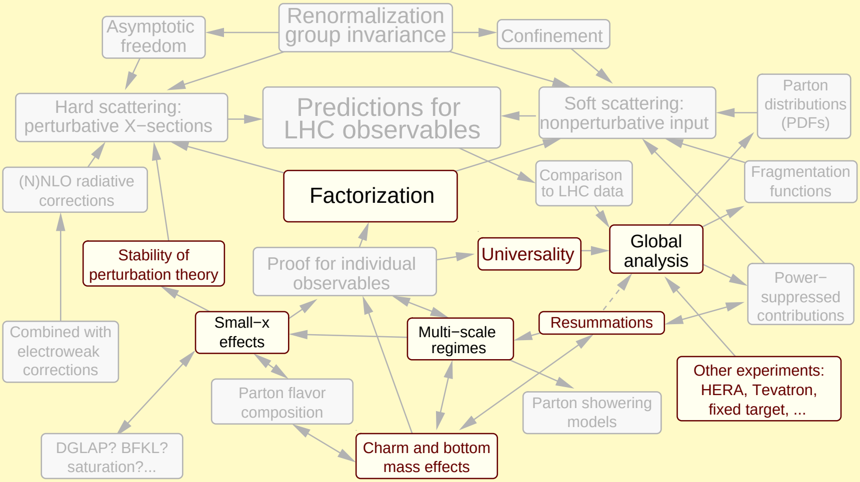

Global interconnections can be as important as (N)NLO perturbative contributions; are different at the Tevatron and LHC

Why QCD at LHC is special

- dominance of sea parton scattering
- small typical momentum fractions x in several key searches (Higgs, lighter superpartners, ...)
- large QCD backgrounds
- complicated event signatures; reliance on differential distributions
- different low-energy dynamics (underlying event, multiple interactions...)
- ...

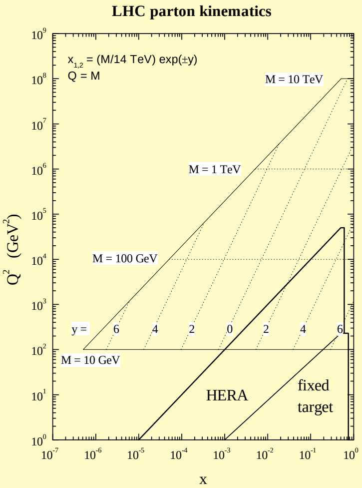

Examples of global connections

- Correlations between collider cross sections through shared parton distribution functions

  based on

  Implications of CTEQ6.6 global analysis for collider observables

  by P. N., Q.-H. Cao, J. Huston, H.-L. Lai, J. Pumplin, D. Stump, W.-K. Tung, C.-P. Yuan; arXiv:0802.0007

- Standard model effects on electroweak precision measurements
  - W boson mass at the Tevatron and LHC

PDF-induced correlations in hadron scattering

- Dependence on the PDF's is strongly correlated for some pairs of cross sections and anti-correlated for other pairs

  ⇒ implications for the monitoring of parton and collider luminosities, determination of new physics parameters

- I will discuss the origin of the correlations, especially for W, Z, $t\bar{t}$ cross sections

Noteworthy (anti)correlations

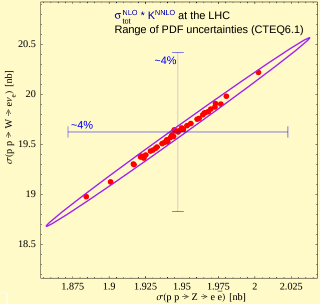

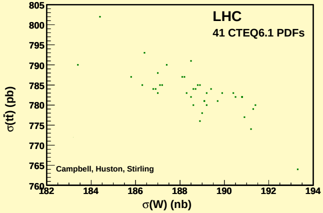

Correlation angle φ

Determines the parametric form of the $X - Y$ correlation ellipse

$$X = X_0 + \Delta X \cos\theta$$
$$Y = Y_0 + \Delta Y \cos(\theta + \varphi)$$

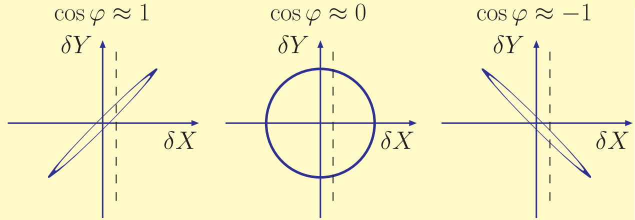

X_0, Y_0: best-fit values

ΔX, ΔY: PDF errors

$\cos\varphi \approx \pm 1$: Measurement of X imposes tight constraints on Y

$\cos\varphi \approx 0$: Measurement of X imposes loose constraints on Y

“Standard candle” processes: W, Z, $t\bar{t}$ production

- Cross sections for $pp \to W^{\pm}X$, $pp \to Z^0 X$ at the LHC can be measured with accuracy $\delta\sigma/\sigma \sim 1\%$ (tens of millions of events even at low luminosity)
- These measurements will be employed to tightly constrain PDF's and monitor the LHC luminosity $\mathcal{L}$ in real time *(Dittmar, Pauss, Zurcher; Khoze, Martin, Orava, Ryskin; Giele, Keller';...)*
  - other methods will initially give $\delta\mathcal{L} = 10 - 20\%$
- $t\bar{t}$ cross section can be potentially measured with accuracy $\approx 5\%$

Theoretical uncertainties on σ_W, σ_Z, $\sigma_{t\bar{t}}$

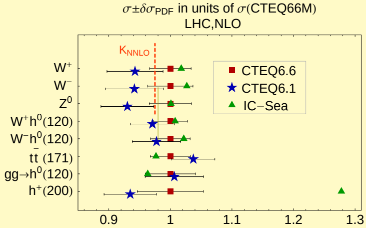

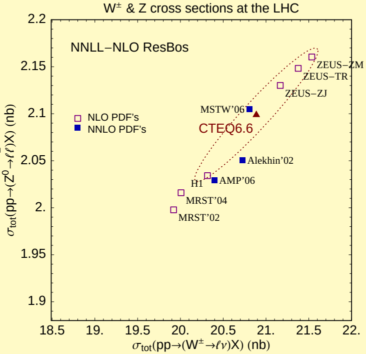

$\sigma_{W,Z}$

► NNLO PQCD: (Hamberg et al; Harlander, Kilgore; Anastasiou et al.): $\sigma_{NNLO} - \sigma_{NLO} = -2\%$

► PDF dependence: $\gtrsim 3\%$ at $\approx 90\%$ c.l.

$\sigma_{t\bar{t}}$

► NLO scale dependence: 11% (to be reduced at NNLO soon)

► m_t dependence: $2 - 3\%$ for $m_t = 172 \pm 1$ GeV

► PDF dependence: 3%

Cross section ratios

- LHC collaborations will normalize many cross sections σ to the "standard candle" cross sections σ_{sc} (i.e., measure $r = \sigma/\sigma_{sc}$)
  - dependence on $\mathcal{L}$ and other systematics may cancel in r
  - PDF uncertainties cancel in r for strongly correlated cross sections; add up in anticorrelated cross sections
- Similar cancellations may occur in $S/\sqrt{B}$, asymmetries, etc.

It helps to find a correlated "standard candle" cross section for each interesting LHC cross section

For example, it is better to normalize σ_{Higgs} to σ_Z ($\sigma_{t\bar{t}}$) if σ_{Higgs} is correlated (anticorrelated) with σ_Z

A mini-poll: Z production at the LHC

Choose all that apply and select the x range

The PDF uncertainty in σ_Z is mostly due to...

1. u, d, $\bar{u}$, $\bar{d}$ PDF's at $x < 10^{-2}$
   ($x > 10^{-2}$)

2. gluon PDF's at $x < 10^{-2}$
   ($x > 10^{-2}$)

3. s, c, b PDF's at $x < 10^{-2}$
   ($x > 10^{-2}$)

An inefficient application of the error analysis

☺ Compute σ_W for 40 (now 44) extreme PDF eigensets

☺ Find eigenparameter(s) producing largest variation(s), such as #9, 10, 30

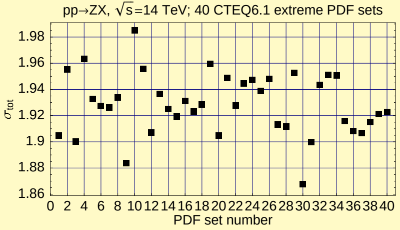

☺ Check that the same eigenparameters produce largest variations in σ_Z

☹ It is not obvious how to relate abstract eigenparameters to physical PDF's $u(x)$, $d(x)$, etc.

CTEQ6.6 theoretical framework

(W.-K. Tung and collaborators)

- A full NLO analysis (NNLO is nearly completed)
- 2700 data points from 35 experiments on DIS, Drell-Yan process, jet production
- Recent improvements in treatment of heavy quark masses in DIS, etc. (CTEQ6.5), with important impact on W, Z cross sections
  - a general-mass factorization scheme with full dependence on $m_{c,b}$
  - free parametrization for strange quarks (constrained by CCFR, NuTeV charged-current DIS data)

General-mass CTEQ6.6 PDF's vs. zero-mass CTEQ6.1 PDF's

Dashes: CTEQ6.1M

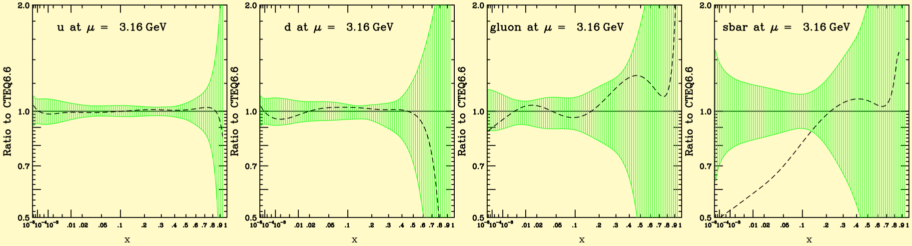

- CTEQ6.6 u, d are above CTEQ6.1 by 2-3% at $x \sim 10^{-3}$; $\therefore$ $\sigma_{W,Z}$ at the LHC larger by $5-6\%$
- very different strange PDF's: $s(x)+\bar{s}(x) \neq \bar{u}(x)+\bar{d}(x)$ at low μ

Multi-dimensional PDF error analysis

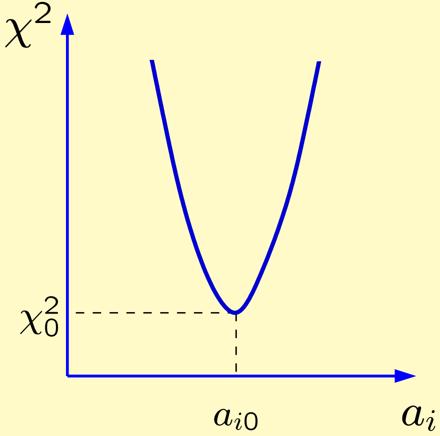

- Minimization of a likelihood function (χ^2) with respect to ~ 30 theoretical (mostly PDF) parameters $\{a_i\}$ and > 100 experimental systematical parameters
  - partly analytical and partly numerical

Multi-dimensional PDF error analysis

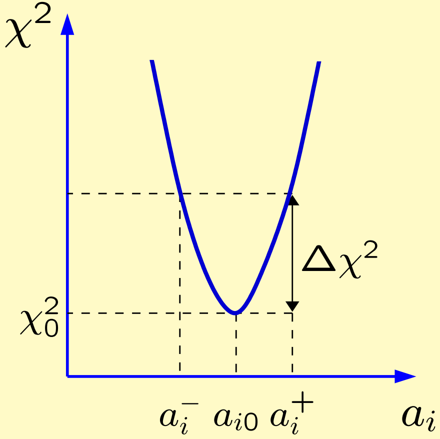

- Establish a confidence region for $\{a_i\}$ for a given tolerated increase in χ^2

Multi-dimensional PDF error analysis

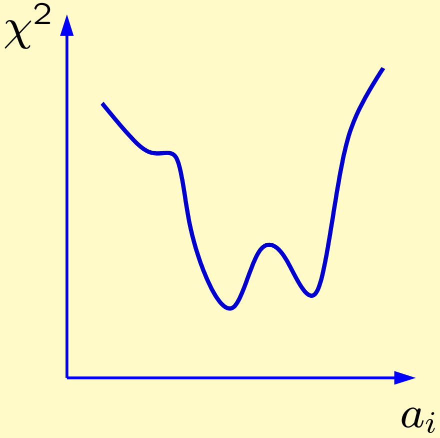

Pitfalls to avoid

- "Landscape"
  - disagreements between the experiments

Multi-dimensional PDF error analysis

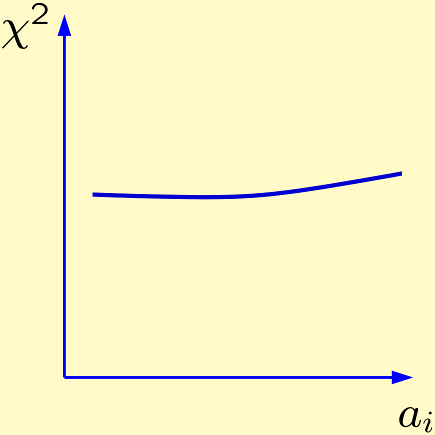

Pitfalls to avoid

- Flat directions
  - unconstrained combinations of PDF parameters

Multi-dimensional PDF error analysis

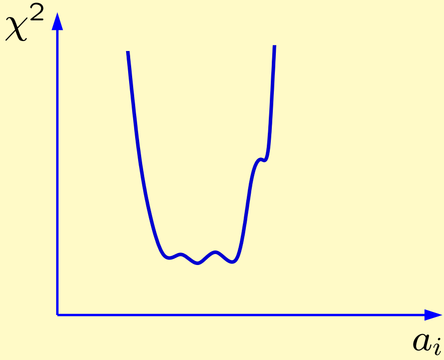

The actual χ^2 function shows

- a well pronounced global minimum χ_0^2
- weak tensions between data sets in the vicinity of χ_0^2 (mini-landscape)
- some dependence on assumptions about flat directions

Multi-dimensional PDF error analysis

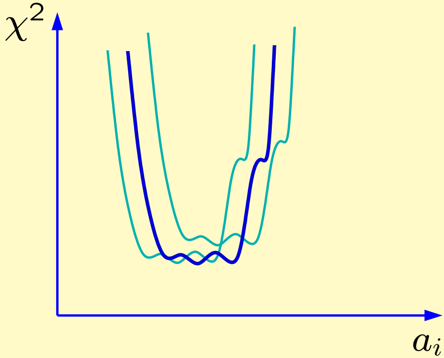

The actual χ^2 function shows

- a well pronounced global minimum χ_0^2
- weak tensions between data sets in the vicinity of χ_0^2 (mini-landscape)
- some dependence on assumptions about flat directions

Multi-dimensional PDF error analysis

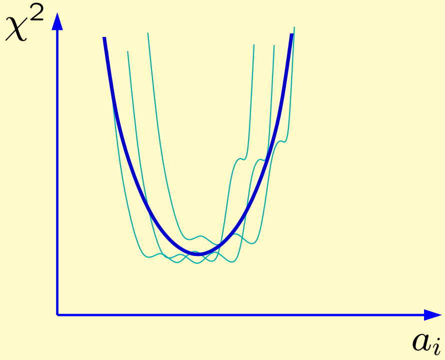

The actual χ^2 function shows

- a well pronounced global minimum χ_0^2
- weak tensions between data sets in the vicinity of χ_0^2 (mini-landscape)
- some dependence on assumptions about flat directions

The likelihood is approximately described by a quadratic χ^2 with a revised tolerance condition $\Delta\chi^2 \leq T^2$

Multi-dimensional PDF error analysis

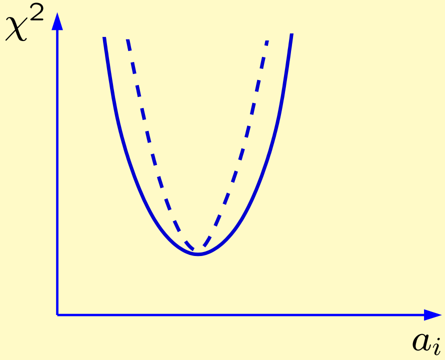

The actual χ^2 function shows

- a well pronounced global minimum χ_0^2
- weak tensions between data sets in the vicinity of χ_0^2 (mini-landscape)
- some dependence on assumptions about flat directions

The likelihood is approximately described by a quadratic χ^2 with a revised tolerance condition $\Delta\chi^2 \leq T^2$

Multi-dimensional PDF error analysis

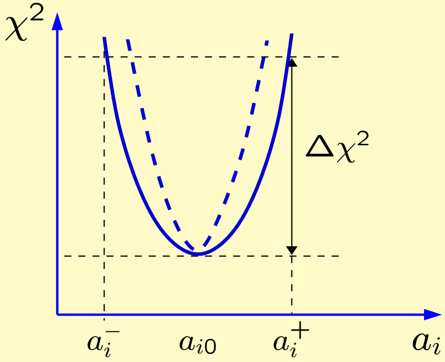

The actual χ^2 function shows

- a well pronounced global minimum χ_0^2
- weak tensions between data sets in the vicinity of χ_0^2 (mini-landscape)
- some dependence on assumptions about flat directions

The likelihood is approximately described by a quadratic χ^2 with a revised tolerance condition $\Delta\chi^2 \leq T^2$

Tolerance hypersphere in the PDF space

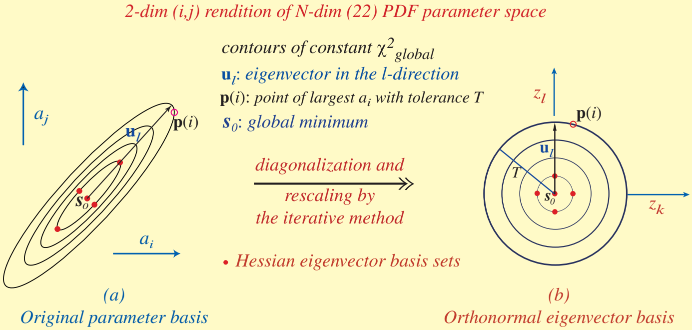

A hyperellipse $\Delta\chi^2 \leq T^2$ in space of N physical PDF parameters $\{a_i\}$ is mapped onto a hypersphere of radius T in space of N orthonormal PDF parameters $\{z_i\}$

Tolerance hypersphere in the PDF space

2-dim (i,j) rendition of N-dim (22) PDF parameter space

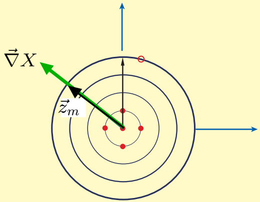

(b)
Orthonormal eigenvector basis

PDF error for a physical observable X is given by

$$\Delta X = \vec{\nabla} X \cdot \vec{z}_m = \left|\vec{\nabla} X\right| = \frac{1}{2}\sqrt{\sum_{i=1}^{N}\left(X_i^{(+)} - X_i^{(-)}\right)^2}$$

Tolerance hypersphere in the PDF space

2-dim (i,j) rendition of N-dim (22) PDF parameter space

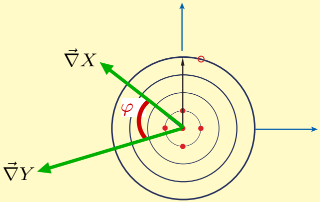

(b)
Orthonormal eigenvector basis

Correlation cosine for observables X and Y:

$$\cos\varphi = \frac{\vec{\nabla}X \cdot \vec{\nabla}Y}{\Delta X \Delta Y} = \frac{1}{4\Delta X\,\Delta Y}\sum_{i=1}^{N}\left(X_i^{(+)} - X_i^{(-)}\right)\left(Y_i^{(+)} - Y_i^{(-)}\right)$$

Correlation angle φ

Determines the parametric form of the $X - Y$ correlation ellipse

$$X = X_0 + \Delta X \cos\theta$$
$$Y = Y_0 + \Delta Y \cos(\theta + \varphi)$$

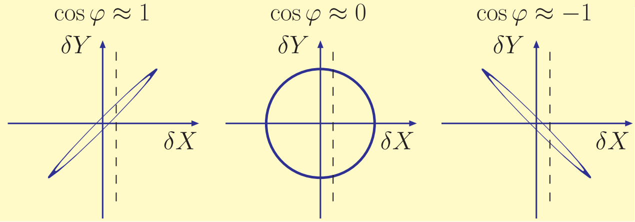

X_0, Y_0: best-fit values

ΔX, ΔY: PDF errors

$\cos\varphi \approx \pm 1$: Measurement of X imposes tight constraints on Y
$\cos\varphi \approx 0$: Measurement of X imposes loose constraints on Y

Types of correlations

X and Y can be

- two PDFs $f_1(x_1, Q_1)$ and $f_2(x_2, Q_2)$ (plotted as $\cos\varphi$ vs x_1 & x_2)
- a physical cross section σ and PDF $f(x, Q)$ (plotted as $\cos\varphi$ vs x)
- two cross sections σ_1 and σ_2

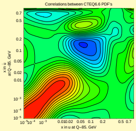

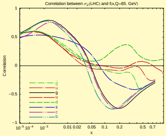

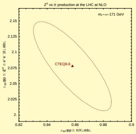

Correlations between $f_1(x_1, Q)$ and $f_2(x_2, Q)$ at $Q = 85$ GeV

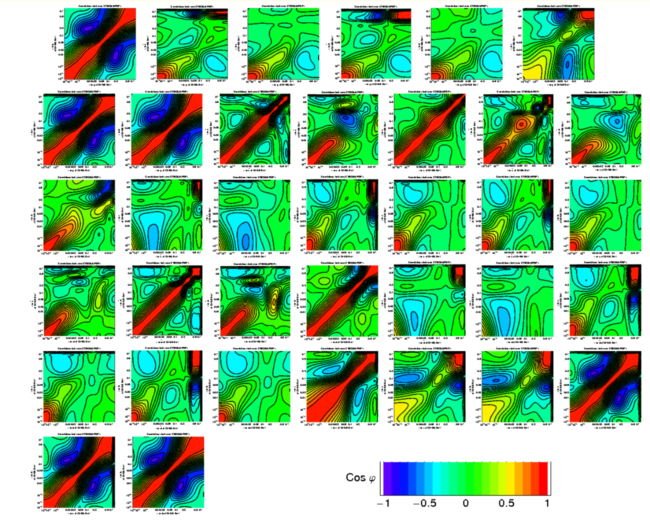

Figures from http://hep.pa.msu.edu/cteq/public/6.6/pdfcorrs/

Correlations between $f(x_1, Q)$ and $f(x_2, Q)$ at $Q = 85$ GeV

$f_1(x_1, Q)$ vs. $f_1(x_2, Q)$

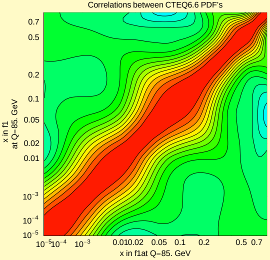

$f_2(x_1, Q)$ vs. $f_2(x_2, Q)$

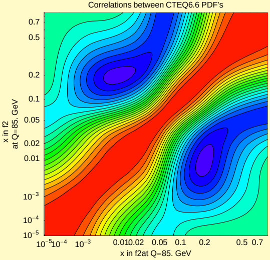

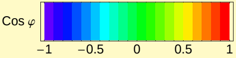

Can you guess which PDF's these are?

Correlations between $f(x_1, Q)$ and $f(x_2, Q)$ at $Q = 85$ GeV

$u(x_1, Q)$ vs. $u(x_2, Q)$

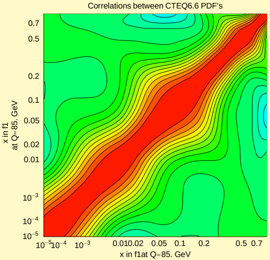

$g(x_1, Q)$ vs. $g(x_2, Q)$

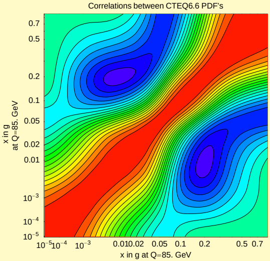

Correlation patterns look similar for g, c, b PDF's (no intrinsic charm here!)

c vs. c

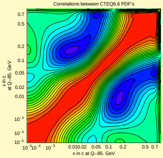

b vs. b

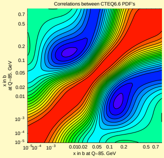

c vs. g

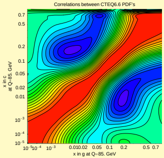

b vs. c

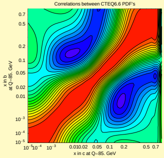

Correlations between $f_1(x_1, Q)$ and $f_2(x_2, Q)$ at $Q = 85$ GeV

d vs u

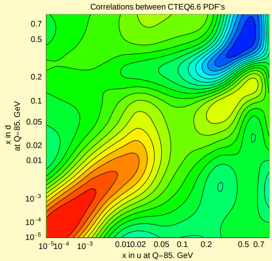

s vs $\bar{u}$ at Q=2 GeV

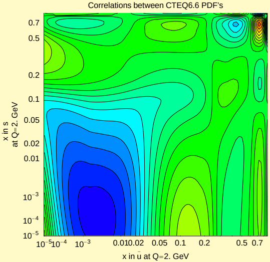

s vs. g

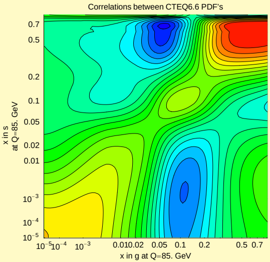

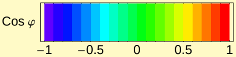

Sometimes there is a clear physics reason behind the correlation (e.g., sum rules or assumed Regge-like behavior); sometimes not

Correlations between $g(x_1, 2 \text{ GeV})$ and $g(x_2, 85 \text{ GeV})$

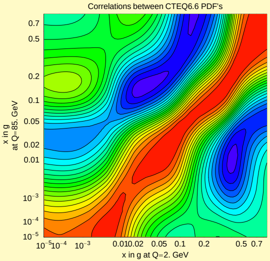

Gluons at $Q = 85$ GeV are correlated with gluons at $Q = 2$ GeV and larger x because of DGLAP evolution

Correlations between *W*, *Z* cross sections and PDF's

Tevatron Run-2

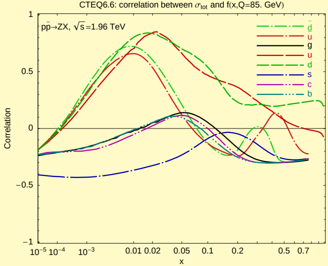

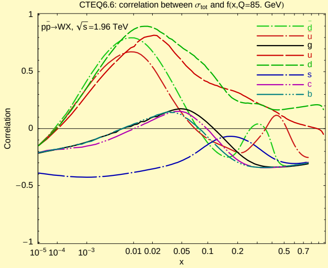

LHC

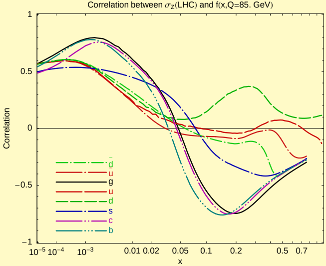

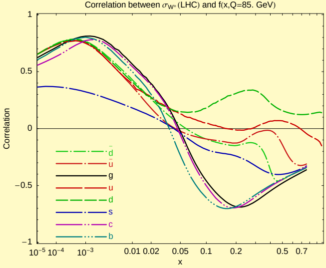

A surprising discovery

LHC Z, W cross sections are strongly correlated with $g(x)$, $c(x)$, $b(x)$ at $x \sim 0.005$

$\therefore$ they are strongly anticorrelated with processes sensitive to $g(x)$ at $x \sim 0.1$ ($t\bar{t}$, $gg \to H$ for $M_H > 300$ GeV)

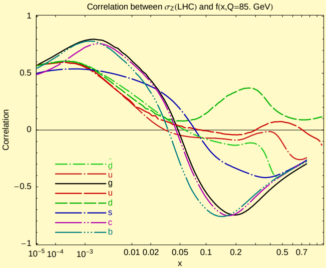

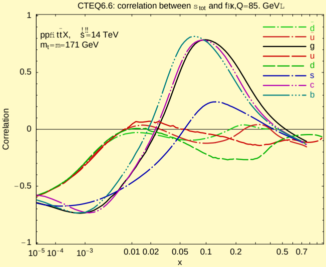

Correlations between $\sigma(gg \to H^0)$, σ_Z, $\sigma_{t\bar{t}}$

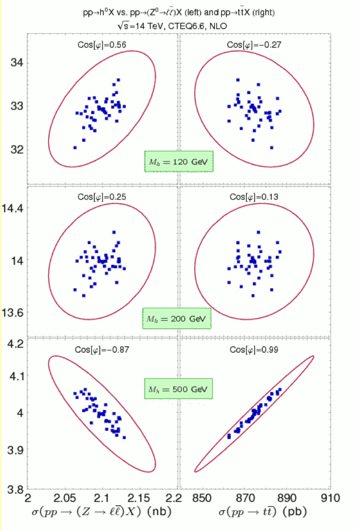

$\cos\varphi$ for various NLO Higgs production cross sections in SM and MSSM

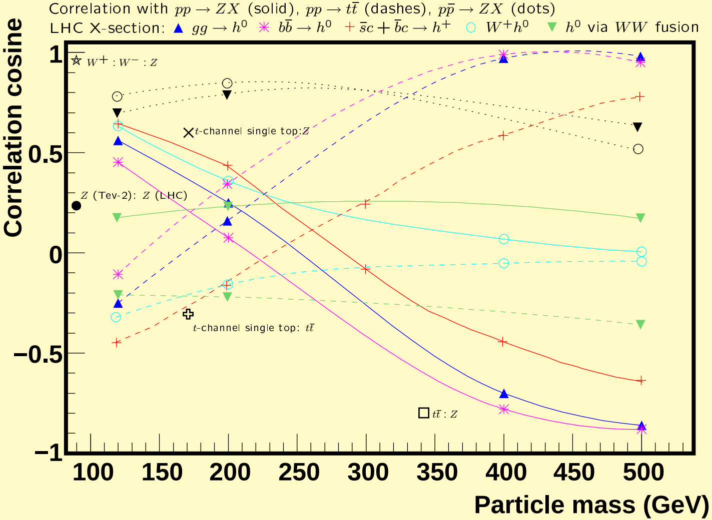

An example of a small correlation with the gluon

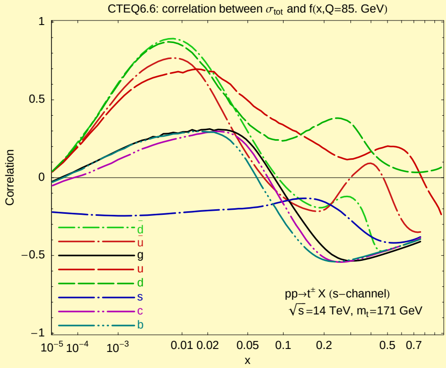

Single-top production (NLO)

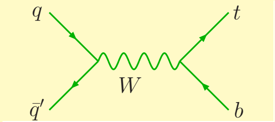

- typical $x \sim 0.01$
- mostly correlated with u, d PDF's

PDF uncertainties in W, Z *total* cross sections are irrelevant for some quark scattering processes (single-top, Z', ...)

Precision tests of electroweak symmetry breaking

Higgs sector in SM and MSSM

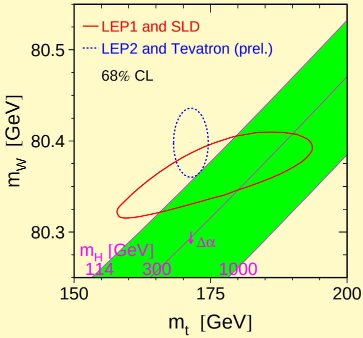

Green band: $114 \leq M_H \leq 1000$ GeV

SM: 1 Higgs doublet, one boson H

- Direct search: $m_H > 114$ GeV at 95% c.l.
- indirect: $M_H = 80^{+39}_{-28}$ GeV at 68% c.l.

MSSM: 2 Higgs doublets; h^0, H^0, A^0, $H^\pm$

$m_h \leq m_Z |\cos 2\beta| + \text{rad. corr.} \lesssim 135$ GeV

- In these models, expect one or more Higgs bosons with mass below 140 GeV
- Many other possibilities for EW symmetry breaking exist!

Higgs sector in SM and MSSM

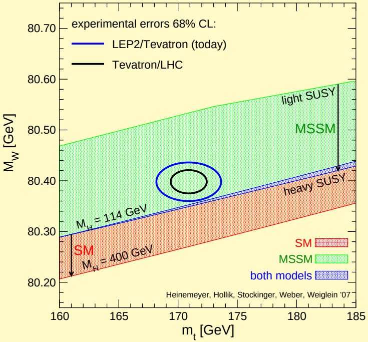

SM band: $114 \leq M_H \leq 400$ GeV
SUSY band: random scan

- the goal of direct and indirect measurements is to over-constrain SM, greatly constrain SUSY
- indirect constraints strongly depend on M_W, m_t values, hence require accurate QCD predictions for W and t production

For example, in SM

$$M_W = 80.3827 - 0.0579 \ln\left(\frac{M_H}{100\text{ GeV}}\right) - 0.008 \ln^2\left(\frac{M_H}{100\text{ GeV}}\right)$$
$$+0.543\left(\left(\frac{m_t}{175\text{ GeV}}\right)^2 - 1\right) - 0.517\left(\frac{\Delta\alpha^{(5)}_{had}(M_Z)}{0.0280} - 1\right) - 0.085\left(\frac{\alpha_s(M_Z)}{0.118} - 1\right)$$

M_W measurement at hadron colliders

- The Tevatron (LHC) collaborations intend to measure M_W with accuracy 15 MeV (5 MeV)
- Several theoretical factors contribute at this level of accuracy
  - NNLO QCD+NLO EW perturbative contributions
  - PDF dependence
  - small-p_T resummation
  - small-x effects
  - dependence on $m_{c,b}$

Measurement of M_W and resummation

The largest QCD uncertainties on M_W arise from

- the model for W boson's recoil in the transverse plane
- parton distributions

$d\sigma/dQ_T$ for W & Z bosons is predicted by the resummation formalism, which evaluates $\sum_{n,m} \alpha_s^n \ln^m(Q_T^2/Q^2)$ at $Q_T \to 0$ to all orders of α_s

(Collins, Soper, Sterman, 1985)

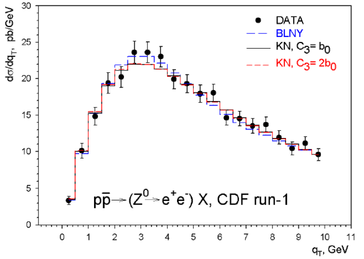

CDF analysis for 207 pb^{-1}:

uncertainty in nonperturbative resummed parameters currently translates into $\delta M_W \approx 3$ MeV (9 MeV) in the $M_T^{\ell\nu}$ (p_T^e) method

QCD factorization at $Q_T \to 0$

(ResBos: C. Balazs, G. Ladinsky, P. N., C.-P. Yuan)

Small-Q_T factorization
$\Lambda^2_{QCD} \ll Q_T^2 \ll Q^2$

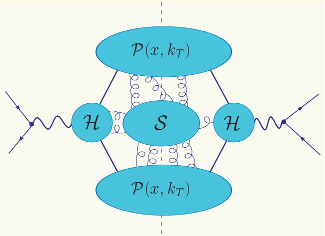

- Realized in space of the impact parameter b (conjugate to Q_T)
- At NNLL accuracy, we include perturbative coefficients up to orders $\mathcal{A}^{(3)}$ (from Moch, Vermaseren, Vogt, 2004); $\mathcal{B}^{(2)}$; and $\mathcal{C}^{(1)}$

$$\left.\frac{d\sigma_{AB\to VX}}{dQ^2\,dy\,dQ_T^2}\right|_{Q_T^2 \ll Q^2} = \sum_{a,b=g,\overset{(-)}{u},\overset{(-)}{d},\dots} \int \frac{d^2 b}{(2\pi)^2} e^{-i\vec{q}_T\cdot\vec{b}}\, \widetilde{W}_{ab}(b, Q, x_A, x_B)$$

$$\widetilde{W}_{ab}(b, Q, x_A, x_B) = |\mathcal{H}_{ab}|^2\, e^{-\mathcal{S}(b,Q)}\,\overline{\mathcal{P}}_a(x_A, b)\,\overline{\mathcal{P}}_b(x_B, b)$$

Universal nonperturbative contributions

A. Konychev, P. N., PLB 633, 710 (2006)

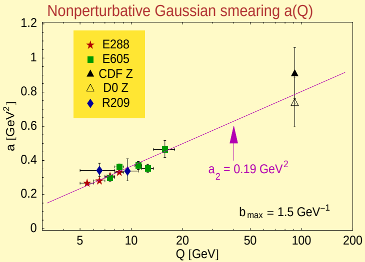

- Q_T factorization: initial-state nonperturbative contributions ($a \sim$"intrinsic" $\langle k_T^2 \rangle/4$) follow a universal quasi-linear dependence on $\ln Q$; this expectation is confirmed by the global analysis of Drell-Yan and Z boson data at $x \gtrsim 0.01$
- the observed $\ln Q$ dependence agrees with the renormalon/lattice estimate *(Tafat)*
- at $Q \sim M_Z$, soft NP corrections dominate over collinear NP corrections
- the model is sufficient to predict many Drell-Yan-like resummed cross sections

Combined analysis of PDF's and resummed nonperturbative function

(Lai, P.N., Pumplin, Tung, Yuan, in progress)

- The common origin of collinear PDF's $f_a(x,\mu)$ and $\mathcal{F}_{NP}(b,Q)$ from k_T-dependent PDF's indicates importance of their simultaneous analysis
  - The best-fit $\mathcal{F}_{NP}(b,Q)$ is correlated with $f_a(x,\mu) \Rightarrow$ consequences for EW precision measurements
  - P_T data constrains poorly known degrees of freedom in $f_a(x,\mu)$
- The technical challenge of including a slow Fourier-Bessel transform into a global fit has been resolved
- The first combined PDF+Q_T fit has been recently finished

Impact on lepton p_T distributions in W boson production

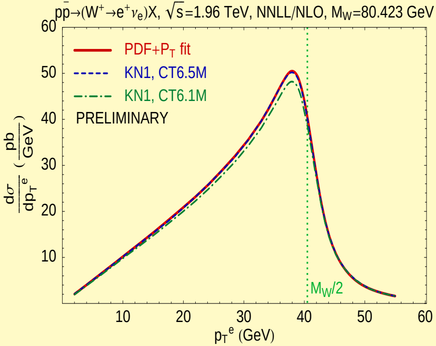

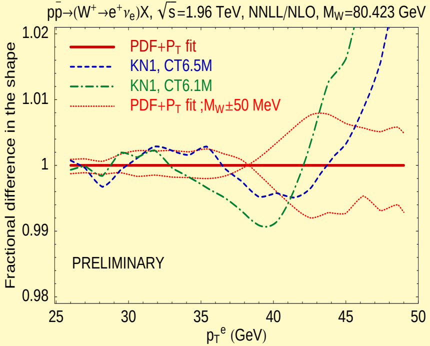

Revised $d\sigma/dp_T^e$ correspond to somewhat larger M_W values extracted from experimental data

Conclusions

- It is exciting to explore rich global connections between the LHC cross sections
  - to calibrate the LHC detectors, monitor LHC luminosity
  - to explore new forms of QCD factorization (resummations) and merge them with important EW contributions
  - to precisely test the Standard Model, understand the EWSB mechanism
  - to impose limits on new physics parameters using hadron collider data

Conclusions (continued)

- Ongoing progress in (N)NLO PQCD global analysis of hadron cross sections
- Correlation analysis in the PDF parameter space is an efficient technique that relates PDF uncertainties in physical cross sections to PDF's for specific parton flavors at known (x, μ)
- This technique is essential for revealing poorly constrained combinations of PDF's, such as those associated with heavy quarks
  - consequences for standard candle and other cross sections at the LHC
  - useful guidance for future LHC measurements aimed at constraining the PDF uncertainties

Backup slides